SEMARAK ILMU PUBLISHING

Journal of Advanced Research in Applied Mechanics

Journal homepage:
https://semarakilmu.com.my/journals/index.php/appl_mech/index
ISSN: 2289-7895

Evaluation of Dendritic Structure of Modified Ductile Ni-Resist

Khairul Ihsan Yaakob[1], Mohd Rashidi Maarof[1,2,*], Muhammad Aminuddin Rosnizan[1], Mohamed Reza Zalani[1], Asnul Hadi Ahmad[1]

[1] Manufacturing Research Focus Group (MFG), Faculty of Mechanical and Automotive Engineering Technology, Universiti Malaysia Pahang (UMP), 26600 Pekan, Pahang, Malaysia
[2] Automotive Engineering Centre, Universiti Malaysia Pahang (UMP), 26600 Pekan, Pahang, Malaysia

ARTICLE INFO

Article history:
Received 29 October 2024
Received in revised form 30 November 2024
Accepted 7 December 2024
Available online 30 December 2024

Keywords:
Metal casting; graphite; Ni-Resist

ABSTRACT

Nowadays, the primary uses of nickel are in batteries, high-temperature applications, and corrosive environments. The use of nickel as the main alloying element has increased as the number of electric and hybrid vehicles has risen. As a result, the price of nickel had reached its maximum and was currently varying to draw in manufacturers. The alloy Ni-Resist is one that is affected. This occurred as a result of nickel being utilized at least 10% of the time as the primary alloying element in Ni-Resist. It is necessary to test other alloying elements in order to lower the percentage. Therefore, in order to lower processing costs, the nickel weight used in this work to create the ductile Ni-resist alloy was decreased. Ten weight percent of nickel and up to twelve weight percent of chromium and manganese were added during the melting process. Subsequently, the influence of the alloying elements was examined concerning its microstructure behavior. After the alloy solidified, the dendritic formation was then characterized in order to assess its size and dimension. Afterwards, the altered alloy was contrasted with traditional ductile iron.

1. Introduction

To compete for market share, product designers and manufacturers nowadays must learn to be competitive. They are also impacted by the ever-accelerating product life cycle. Extensive research was done on new alloy types or by altering it to ensure its manufacturing sustainability in order to stay competitive. This phase will ensure that the part can withstand abrasive and demanding conditions. Some alloys, such as Ni-Resist alloy, which is primarily used for dynamic load at high temperatures, have been impacted by the recent research.

The main austenite structure (instead of ferrite or pearlite) and graphite nodules (instead of flake graphite) are two main structural components of the Ductile Ni-Resist (DNR) alloy. Its exceptional machinability, high strength-to-weight ratio, and generally good mechanical properties at high temperatures are all a result of these characteristics. Because it has an austenitic matrix at all

* *Corresponding author.*
E-mail address: mrashidi@umpsa.edu.my

https://doi.org/10.37934/aram.130.1.159167

temperatures, this material was created and is appropriate for high temperature applications. In contrast, there is a critical temperature range for conventional cast iron and steel applications.

At 675^{o}C, the crystal structure changes from Body-Centered Cubic BCC to Face-Centered Cubic FCC, which frequently results in castings breaking and distorting. Austenitic structures have never experienced these problems.

This phenomenon is caused by changes in volume that arise from matrix phase shifts between austenite and ferrite. Because DNR alloys do not undergo this transformation and maintain an austenitic matrix at all temperatures, they are beneficial for high temperature applications. It is achieved by properly alloying base iron during the material casting process. When alloying elements are added appropriately, the Time-Temperature-Transformation (T-T-T) curve is usually shifted to the right, avoiding the "nose" of the T-T-T curve [1]. After allowing the molten metal to solidify during the alloying phase, an austenite microstructure can form and maintain its structure at room temperature. This process does not use any heat treatment at all. Owing to these exceptional properties, DNR alloy can be melted and alloyed at a lower melting point (roughly 1200–1400^{o}C) in oil, gas, and power plant applications than austenitic steel (roughly 1400^{o}C and above) [2]. From a manufacturing standpoint, the temperature variations offer flexible control over the elevated temperature of molten metal as well as advantageous electricity usage.

A recent study indicates that nickel (Ni) is an effective primary alloying element for the DNR alloy processing. The process is influenced by Ni, which is present in the metal composition and acts as an austenite matrix stabilizer. This results in the emergence of the as-cast austenite microstructure in the DNR alloy. Ni suppresses the austenite (γ) → ferrite (α) transition into conventional ductile iron by at least 18 weight percent [3]. Nickel is an expensive material to use, even though it is effective at converting the iron phase into an austenite structure. Due to the high cost of Ni, which is a known to be a relatively expensive raw material, alloying DNR alloy is economically limited. In an effort to reduce production costs, studies have been done to decrease the Ni/wt% in the overall composition of DNR alloys. In order to effectively convert alloyed iron to austenite structure, an attempt was made to apply as little as thirteen weight percent of Ni/wt% [4]. The attempt was made by combining other alloys while they were melting. Manganese (Mn) and copper are potential alloying elements that can replace DNR alloying element; the outcomes of this substitution have been reported in another study. However, the experiment's results showed a mixed reaction. Morrison [3] argues that while copper can form an austenite structure, the shape of the nodule graphite in the DNR alloy is negatively impacted by this process. As the nodule solidified, its shape changed. In the meantime, Mn, a distinct candidate, stabilizes austenite and concurrently encourages the formation of carbides rather than the necessary free graphite. Morrison added that an alloy is only contributed towards free carbide DNR alloy if, at the time of alloying, it contains less than 4 weight percent Mn.

As was previously mentioned, free graphite will not immediately solidify into the shape of nodule graphite when more manganese is added during alloying. Instead, it encourages carbide formation. It is advised to use an inoculation technique to lessen the production of carbide. As proposed by Jincheng [5], inoculation has been reported to considerably improve the distribution and graphite form of conventional ductile iron. Additionally, it has been reported by Choi *et al.,* [6] that inoculation amplifies the undercooling effect that occurs during the casting solidification of traditional cast iron. Therefore, there is a lower likelihood of carbide forming during solidification as opposed to graphite nodules. Similarly, he suggested that inoculation can generally improve the distribution and form of graphite in conventional ductile iron. In their investigation, inoculation is proposed as a potential solution to augment the undercooling effect during casting solidification. According to Jiyang's [7] research, the cooling curve can minimize the undercooling zone throughout the solidification process by optimizing the material structure. As a result, there is less time for the formation of dendritic

structure and less opportunity for grain boundaries to widen during solidification. Consequently, less room will exist for carbide to form at the grain boundary. The technique makes it possible to track the undercooling phenomenon using solidification cooling curves. As a result, the segregation factor and the area that solidifies last are decreased. Regarding the impact of the modifying alloy on the modified DNR alloy dendritic structure with a higher manganese weight percentage, however, fewer studies have been published.

The austenitic region, for steel or iron, is an interesting topic. Boilers, turbochargers, and exhaust system components are a few examples of applications where the austenitic zone forms and remains stable at room and elevated temperatures. This is why scientists are keen to alloy steel or iron with a specific composition in order to maintain the austenitic zone to any temperature, including high temperatures. Because most researchers concentrated more on austenitic steel than austenitic iron, the literature on corrosion of DNR austenitic matrix alloy is generally limited. This occurs because iron is produced more on a customized basis, whereas steel can be melted at a higher volume in bulk. It was found by Anderson and Vanessa [8] that oxidation resistance happens between 600 and 900 oC when the composition and scale morphology of the Fe-Mn-Al-Si alloy are examined. The existence of an extra phase (oxides of Al, Mn, and Fe) after the oxidation test is what results in the moderate oxidation resistance. Tjong [9] looked into the possibility of using Mn in place of Cr and Ni to produce FeAlMnC. In his research, he observed mechanical properties that are achievable at cryogenic temperatures. An increased manganese content DNR alloy was modified, and Rashidi and Hasbullah [10] examined its mechanical characteristics and microstructure. The analysis found that an austenitic structure could be achieved in the alloy. The oxidation test was not performed, though. Heat-resistant Si-Mo ductile cast iron's mechanical characteristics and oxidation resistance were examined by Kim *et al.,* [11]. The findings demonstrated that the alloy can be improved by changing certain alloy elements.

The goal of this study is to create a modified DNR alloy by combining both Ni and Mn at a specific composition. While Ni/wt% falls to as low as 10 wt%, Mn/wt% increases to as high as 12 wt%. An austenite structure and a graphite nodule should be present in the microstructure of the modified alloy. The impact of a high manganese weight percentage alloy on the modified DNR alloy's austenitic dendritic structure is investigated. The objective is to comprehend the relationship between the microstructural inhomogeneity of the casting and the dendritic dimension of the modified DNR alloy. The emphasis is considered significant because microstructure, particularly the dendritic structure, directly imparted to the properties of DNR alloys.

2. Methodology

An induction furnace with a 50 kg holding capacity, 200 kW of power, and a frequency range of 1000–3000 Hz was used to conduct the current investigation. The following charge materials (steel scrap, pig iron, and pure nickel) were used to create modified DNR alloy with the desired composition: (a) 9Mn-10Ni; (b) 10Mn-10Ni; (c) 11Mn-10Ni; and (d) 12Mn-10Ni wt%. According to Rashidi and Hasbullah [10], ferro-manganese (FeMn) and ferro-chrome (FeCr) were added following stirring sessions to increase the content of manganese and chromium. In order to make a green sand mold, bentonite, water, and silica sand were mixed together. The in-mould technique was used for both the magnesium treatment and the inoculation. With a weight percentage of 1.1 in the mold reaction chamber, FeSiMg—a magnesium-containing material with a sizing of approximately 1-4 mm—was added [10]. The melt was cleaned and superheated to 1500+20^{o}C before it was poured into a mold at 1400+20^{o}C. As illustrated in Figure 1, the inoculant was added to the mold reaction chamber at a weight percentage of 0.5 after the nodulant had been covered in molten metal. Table

1 lists the chemical compositions of all varieties of experimental nickel, iron, FeMn, FeCr, nodularizer, and inoculant. The nodulant and inoculant were introduced into a well-built chamber in each casting's runner system. There was a 120 mm gap between the in-gate location and the reaction chamber design. An inoculant with a grading size of 0.2 to 0.7 mm was utilized in order to minimize fading and encourage inoculant dissolution. Test specimens from ASTM A439 Y-blocks were sectioned, grounded, and polished using 0.3 µm alumina powder in order to obtain microstructural specimens. The dimensions of the second set of sample coupons were cut to 15.0 x 15.0 x 2.0 mm. They were mechanically ground to 2400 mesh on SiC paper and then polished with 1.0 µm diamond paste. The samples were polished to a mirror shine and then cleaned with ultrasonic agitation for ten minutes in ethanol and acetone. The samples were dried and stored in a desiccator prior to being exposed. Following microstructure characterization by scanning electron microscopy (SEM), the specimens' chemical compositions were examined using X-ray energy dispersive spectroscopy (EDS). The chemical analysis was carried out using the EDS model Philips XL40 system.

Fig. 1. Experimental setup during molten metal pouring

Table 1
Chemical composition of iron, alloyed materials, nodularizer, inoculant, FeMn and FeCr (wt %)

	Element										
	C	Si	Mn	P	S	Mg	Ni	Ca	Cr	R.E	Fe
Pig iron	2.91	2.28	0.12	0.07	0.02	-	0.02	-	-	-	Balance
Steel	0.20	0.15	0.60	0.03	0.02	-	-	-	-	-	Balance
Nickel	-	-	-	-	-	-	99.00	-	-	-	Balance
FeMn	-	1.00	86.00	0.10	0.02	-	-	-	-	-	-
FeCr	8.00	4.00	-	0.04	0.04	-	-	-	60.0	-	-
Nodularizer	-	44.00	-	-	-	5.00	-	2.00	-	1.90	-
Inoculant	-	70.00	-	-	-	-	-	2.00	-	-	Balance

3. Results

3.1 Microstructure Evaluation

During the casting process, an alloy with a hypoeutectic composition was created, comprising various component alloys with Fe, C, Si, Mn, Ni, and other elements. Segregation, element solubility, and phase formation were a few of the processes involved in solidification. This alloyed iron is made up of several phases, including carbides, graphite aggregate, eutectic austenite, austenite matrix, and impurity inclusion, according to further analysis [12]. None of the specimens' graphite forms seem to be fully nodular. Additionally, a flake graphite microstructure was found, which had an impact on how much of the nodule graphite shape was overall. The graphite of modified DNR alloy was found to be less spherical than that of common ductile iron, as indicated by these results (Figure 2).

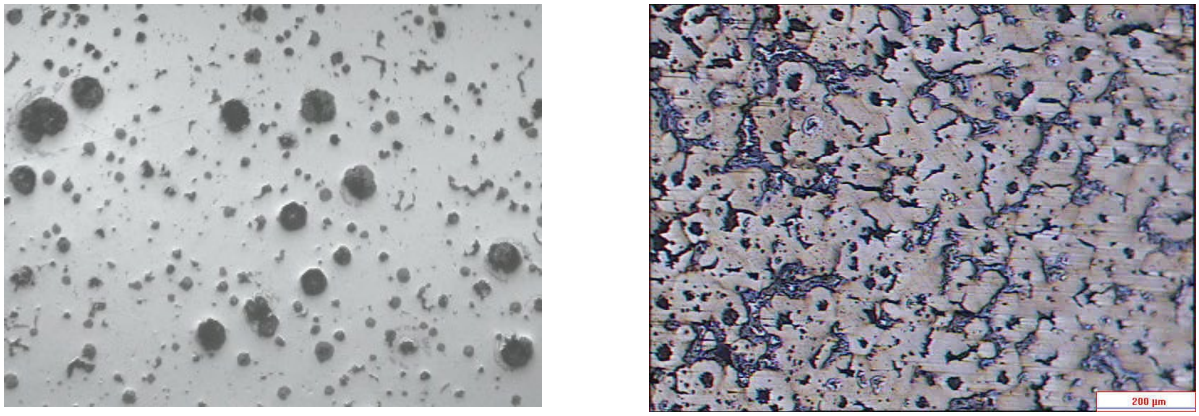

(a) (b)

Fig. 2. Distribution of nodule graphite shape in alloyed grain (a) by microscope iron and (b) by SEM micrograph

According to a qualitative investigation using microstructure analysis, 1.0% and above of magnesium treatment is the appropriate percentage to convert graphite shape. Before the casting was allowed to solidify, the magnesium treatment method was added to change the flake-shaped graphite into a nodule-shaped material. The nodule's parameter size was divided into groups of one to ten micrometers, ten to twenty micrometers, and so on.

The discrete structures that emerge from the graphite nodules within the sample suggest that the production of graphite took place during the casting or solidification process. The size, shape, and distribution of these nodules can vary, adding to the overall microstructure of the material. The process of solidification which was influenced by magnesium treatment, in which the carbon in the molten metal separates and crystallizes into graphite structures, is most likely what causes the graphite nodules [13]. Nonetheless, a semi-spheroidal structure observed in some of these graphite nodules suggests that they are incomplete growth. This suggests that either the growth of these graphite structures was stopped during solidification, or the graphite development process may not have been completed, or the modified DNR alloy altered the overall solidification process compared to conventional iron [14].

The provided fracture images (Figure 3) show the evaluation of microstructures using a scanning electron microscope (SEM). Three images were captured at different magnifications: image a) at 50x, image b) at 200x, and image c) at 500x. Upon closer inspection, these images show that the microstructure contains dendrites. Within the observation are dendrites, which are branching structures resembling tree or fern formations. The terms secondary arm spacing (SDAS) and dendritic arm spacing (DAS) refer to the microstructural characteristics of dendritic growth patterns [15].

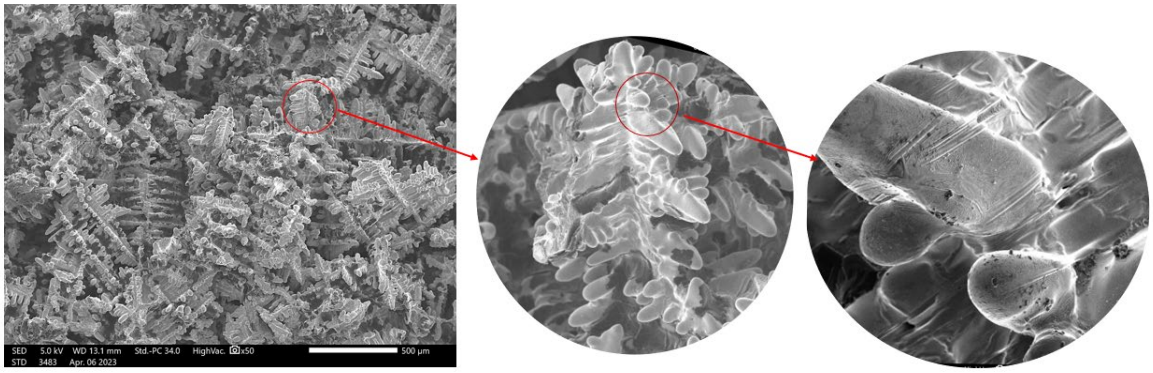

Fig. 3. Distribution of DAS and SDAS structure revealed by SEM micrograph (a) macro view of macrostructure, (b) close up showing DAS structure and (c) close up at higher magnification identifying SDAS morphology

The distance between a dendritic structure's individual arms or branches is referred to as dendritic arm spacing. It shows the typical distance between neighbouring dendritic network arms. A number of variables, including the material's composition, processing conditions, and rate of cooling, affect DAS. Dendrite arm spacing generally increases with slower cooling rates and decreases with faster cooling rates. The terms secondary arm spacing (SDAS) and dendritic arm spacing (DAS) refer to the microstructural characteristics of dendritic growth patterns (Figure 4). The distance between a dendritic structure's individual arms or branches is referred to as dendritic arm spacing. It shows the typical distance between neighbouring dendritic network arms. A number of variables, including the material's composition, processing conditions, and rate of cooling, affect DAS [16]. Dendrite arm spacing generally increases with slower cooling rates and decreases with faster cooling rates.

The SEM micrograph was used to measure and observe the size of DAS. The average dimension is found to be between 200 and 300 µm, which is relatively large (Figure 5). The SDAS structure shown in Figure 6 is comparable in this regard. In this study, the SDAS size ranges from 20 to 28 µm. This indicates that the solidification process is proceeding very slowly overall, which is conducive to the undercooling phase occurring (Figure 7). Ultimately, this allowed the structure of the DAS and SDAS to expand [17]. Higher porosity was anticipated to be trapped with this microstructure in this dimension after solidification was complete. Figure 4's observations, which demonstrate a great deal of porosity, void, and free graphite trapped between the DAS and SDAS structure, provide evidence for this. The smaller DAS structure will trap less porosity, so theoretically, this structure is probably weaker than the smaller one. Future property testing of this hypothesis is necessary.

The temperature gradient in the liquid (GL) and the solidification front velocity (R) are related to the formation of dendritic structure. With latent heat flows into both solid and liquid, the comparatively lower ratio of GL to R resulted in a negative GL. There was an unstable planar interface. Dendritic protuberances quickly grew into the liquid that was undercooling and absorbed the latent heat they were accumulating. This condition is closely associated with the coring phenomenon that happens during the undercooling phase and cellular morphology as summarized by Sangame *et al.,* [14].

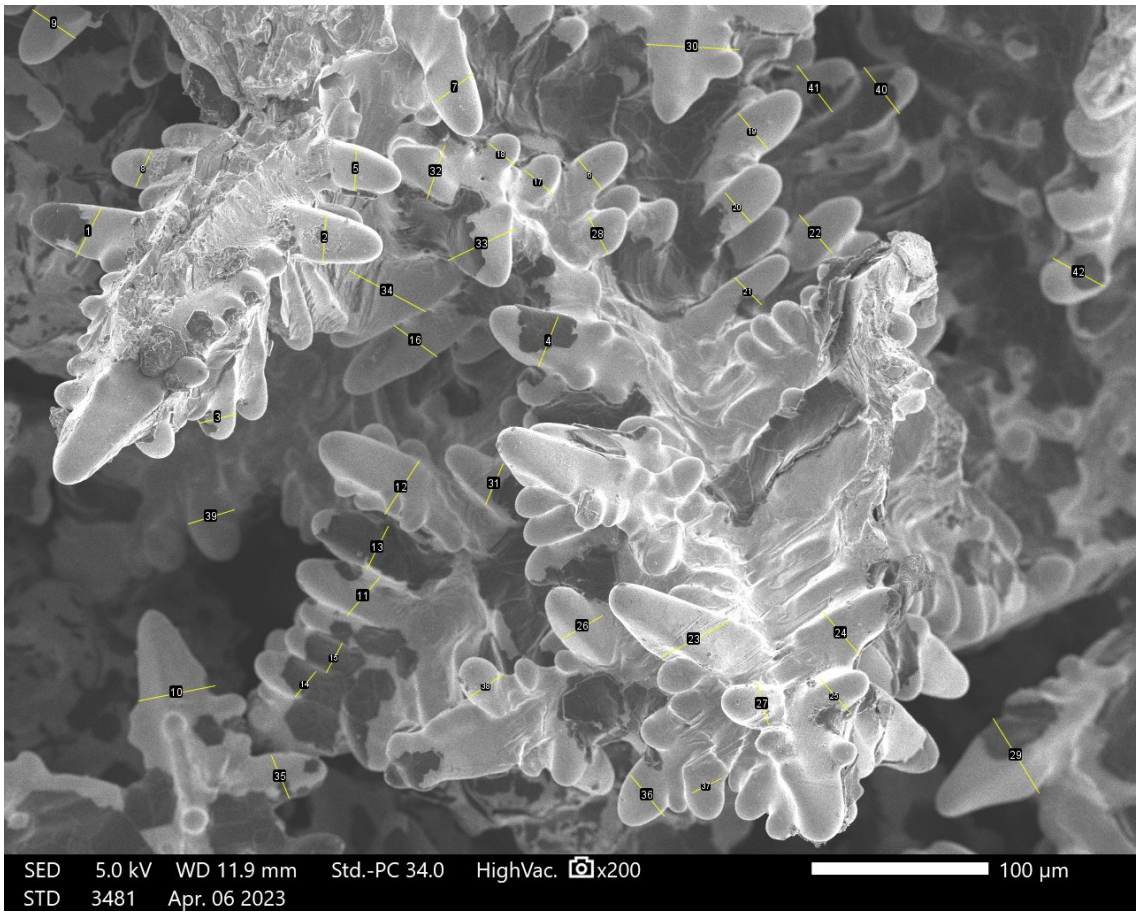

Fig. 4. Closer view of the microstructure at higher magnification, displaying the modified DNR alloyed overall DAS and SDAS structure

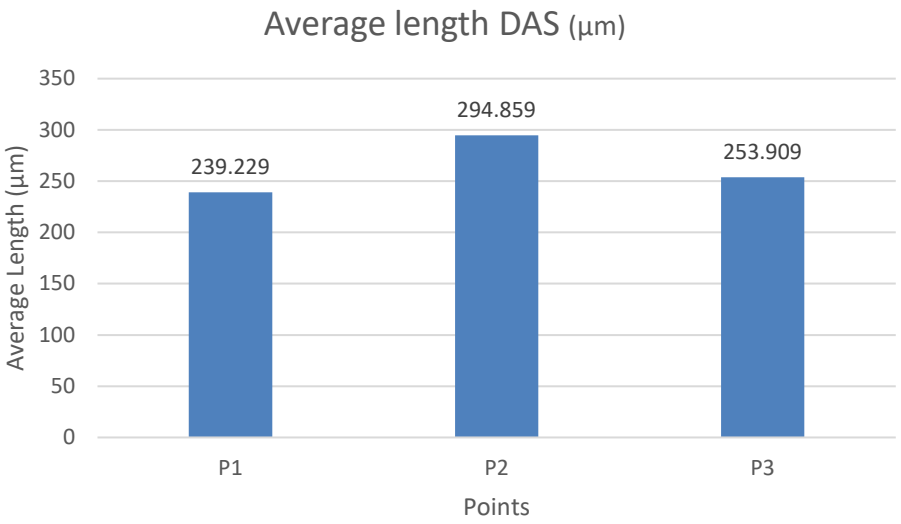

Fig. 5. Average length of DAS structure

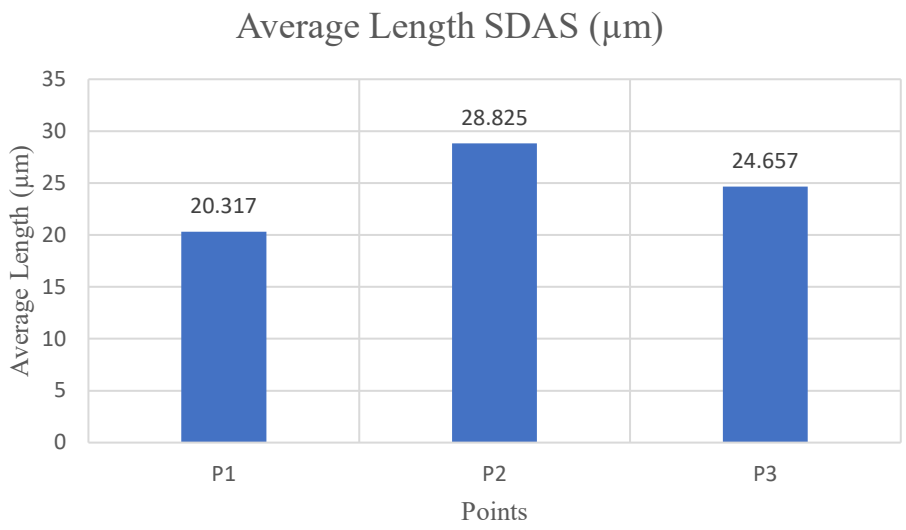

Fig. 6. Average length of SDAS structure

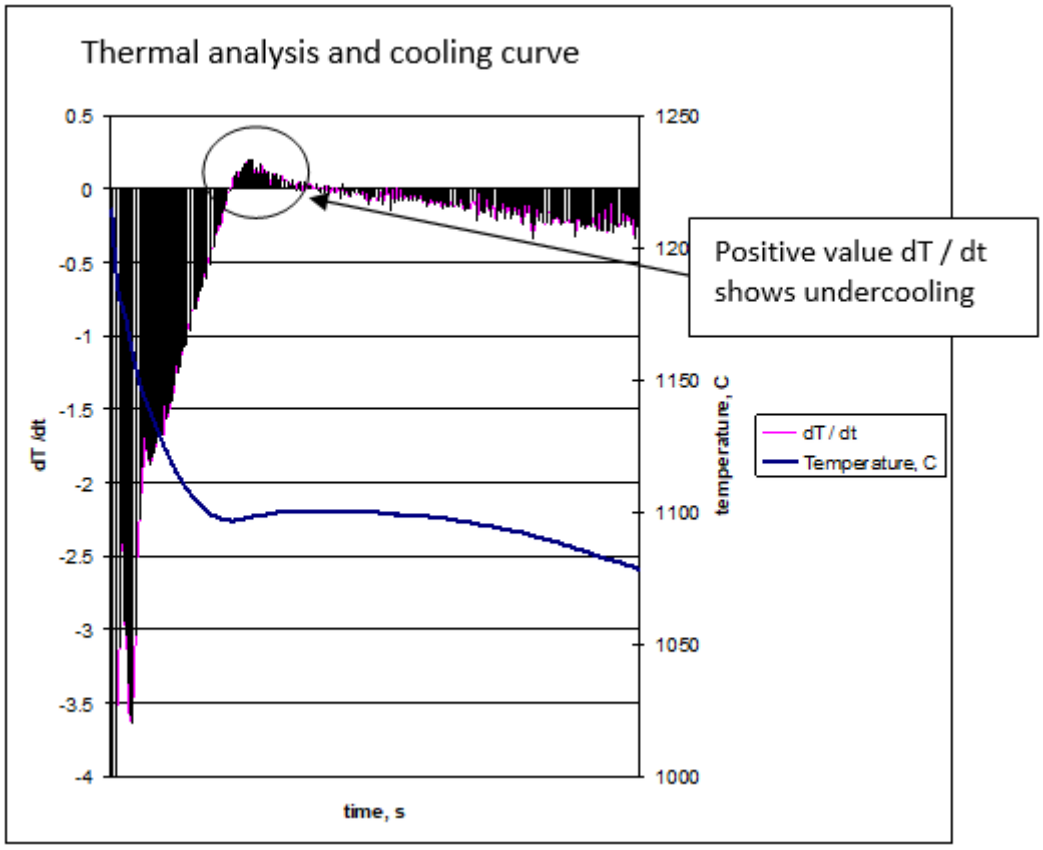

Fig. 7. Thermal analysis and cooling curve of modified DNR alloy solidification

4. Conclusions

The assessment and development of DAS and SDAS structure sizes and dimensions in an alloyed iron are discussed in this paper. Instead of being in the form of untreated flake, the dendritic formation immediately following the magnesium treatment was allowed to solidify to room temperature and contained nodule graphite shape. Despite sharing a nearly identical pattern, the size of those dendritic structures is average. Most of the measurements appeared as 200–300 µm

sizes. A porosity, void, and free graphite that became trapped during the solidification phase were present next to this DAS and SDAS structure.

Acknowledgement
This research was funded by a grant from Ministry of Higher Education of Malaysia (FRGS Grant FRGS/1/2022/TK10/UMP/02/64 - RDU220135) and university's internal grant (RDU220305).

References

[1] Çelik, Gülşah Aktaş, Maria-Ioanna T. Tzini, Şeyda Polat, Ş. Hakan Atapek, and Gregory N. Haidemenopoulos. "Thermal and microstructural characterization of a novel ductile cast iron modified by aluminum addition." *International Journal of Minerals, Metallurgy and Materials* 27 (2020): 190-199. https://doi.org/10.1007/s12613-019-1876-8

[2] Xiang, Shengmei, Stefan Jonsson, Baohua Zhu, and Joakim Odqvist. "Corrosion fatigue of austenitic cast iron Ni-Resist D5S and austenitic cast steel HK30 in argon and synthetic diesel exhaust at 800° C." *International Journal of Fatigue* 132 (2020): 105396. https://doi.org/10.1016/j.ijfatigue.2019.105396

[3] Morrison, J. C. "Corrosion behaviour of Ni-Resist cast irons." *Anti-Corrosion Methods and Materials* 30, no. 8 (1983): 8-9. https://doi.org/10.1108/eb007227

[4] Fatahalla, Nabil, Aly AbuElEzz, and Moenes Semeida. "C, Si and Ni as alloying elements to vary carbon equivalent of austenitic ductile cast iron: Microstructure and mechanical properties." *Materials Science and Engineering: A* 504, no. 1-2 (2009): 81-89. https://doi.org/10.1016/j.msea.2008.10.019

[5] Jincheng, Xu. "Ecodesign for wear resistant ductile cast iron with medium manganese content." *Materials & Design* 24, no. 1 (2003): 63-68. https://doi.org/10.1016/S0261-3069(02)00076-6

[6] Choi, J. O., J. Y. Kim, C. O. Choi, J. K. Kim, and P. K. Rohatgi. "Effect of rare earth element on microstructure formation and mechanical properties of thin wall ductile iron castings." *Materials Science and Engineering: A* 383, no. 2 (2004): 323-333. https://doi.org/10.1016/j.msea.2004.04.060

[7] Jiyang, Zhou. "Colour metallography of cast iron." *China foundry* 6, no. 1 (2009): 57-69.

[8] Dias, Anderson, and Vanessa de Freitas Cunha Lins. "Scale morphologies and compositions of an iron-manganese-aluminum-silicon alloy oxidated at high temperatures." *Corrosion science* 40, no. 2-3 (1998): 271-280. https://doi.org/10.1016/S0010-938X(97)00134-0

[9] Tjong, S. C. "Electron microscope observations of phase decompositions in an austenitic Fe-8.7 Al-29.7 Mn-1.04 C alloy." *Materials Characterization* 24, no. 3 (1990): 275-292. https://doi.org/10.1016/1044-5803(90)90055-O

[10] Rashidi, Maarof Mohd, and Mohd Hasbullah Idris. "Microstructure and mechanical properties of modified ductile Ni-resist with higher manganese content." *Materials Science and Engineering: A* 574 (2013): 226-234. https://doi.org/10.1016/j.msea.2013.02.038

[11] Kim, Yoon-Jun, Ho Jang, and Yong-Jun Oh. "High-temperature low-cycle fatigue property of heat-resistant ductile-cast irons." *Metallurgical and Materials Transactions A* 40 (2009): 2087-2097. https://doi.org/10.1007/s11661-009-9911-4

[12] Stan, Iuliana, Denisa-Elena Anca, Iulian Riposan, and Stelian Stan. "Solidification pattern of 4.5% Si ductile iron in metal mould versus sand mould castings." *Journal of Thermal Analysis and Calorimetry* 148, no. 5 (2023): 1805-1817. https://doi.org/10.1007/s10973-022-11832-4

[13] Mrvar, Primož, Mitja Petrič, and Milan Terčelj. "Thermal Fatigue of Spheroidal Graphite Cast Iron." In *TMS Annual Meeting & Exhibition*, pp. 406-415. Cham: Springer Nature Switzerland, 2023. https://doi.org/10.1007/978-3-031-22524-6_37

[14] Sangame, Bahubali Babanrao, Y. Prasannatha Reddy, and Vasudev D. Shinde. "Analyzing the effect of inoculant addition on the solidification of ductile cast irons using thermal analysis." *World Journal of Engineering* ahead-of-print (2022). https://doi.org/10.1108/WJE-07-2022-0272

[15] Bauer, Branko, Ivana Mihalic Pokopec, Mitja Petrič, and Primož Mrvar. "Effect of bismuth on preventing chunky graphite in high-silicon ductile iron castings." *International Journal of Metalcasting* 14 (2020): 1052-1062. https://doi.org/10.1007/s40962-020-00419-0

[16] Liu, Jin-hai, Jian-shuai Yan, Xue-bo Zhao, Bin-guo Fu, Hai-tao Xue, Gui-xian Zhang, and Peng-hui Yang. "Precipitation and evolution of nodular graphite during solidification process of ductile iron." *China Foundry* 17 (2020): 260-271. https://doi.org/10.1007/s41230-020-0042-2

[17] Chatcharit, Kiattisaksri, Akira Sugiyama, Kohei Morishita, Taka Narumi, Kentaro Kajiwara, and Hideyuki Yasuda. "Time evolution of solidification structure in ductile cast iron with hypereutectic compositions." *International Journal of Metalcasting* 14 (2020): 794-801. https://doi.org/10.1007/s40962-020-00424-3